Available online at www.sciencedirect.com
ScienceDirect
International Journal of Machine Tools & Manufacture 47 (2007) 985–995
INTERNATIONAL JOURNAL OF MACHINE TOOLS & MANUFACTURE DESIGN, RESEARCH AND APPLICATION
www.elsevier.com/locate/ijmactool

Improving accuracy through shrinkage modelling by using Taguchi method in selective laser sintering

N. Raghunath, Pulak M. Pandey*

Department of Mechanical Engineering, Indian Institute of Technology Delhi, New Delhi, India

Received 10 March 2006; received in revised form 4 July 2006; accepted 5 July 2006
Available online 7 September 2006

Abstract

Selective laser sintering (SLS) is a powder-based rapid prototyping process in which parts are built by selective sintering of layers of powder using CO_2 laser. Nowadays, SLS is emerging as a rapid manufacturing technique, which produces functional parts in small batches, particularly in aerospace application and rapid tooling. Therefore, SLS prototypes should have high accuracy in order to satisfy functional requirements. Shrinkage is one of the major factors which influence the accuracy of the SLS parts. To compensate for shrinkage, the material shrinkage coefficient or scaling factor is to be calculated in each direction and is to be applied to STL file. The amount of shrinkage encountered is found to be governed by the process parameters during processing and cannot be kept constant as it is a usual practice in today's SLS technology. In the present work, the relationship between shrinkage and the various process parameters namely laser power, beam speed, hatch spacing, part bed temperature and scan length in SLS have been investigated. Cuboids with suitable dimensions are fabricated rather than fabricating long parts along X, Y and Z directions in order to study shrinkage as it is expected that the shrinkage along X, Y and Z direction is not independent. Optimum shrinkage conditions are obtained by maximizing signal-to-noise (S/N) ratio and analysis of variance (ANOVA) is used to understand the significance of process variables affecting shrinkage. Laser power and scan length are found to be most significant process variables influencing shrinkage in X- direction. Along Y-direction laser power and beam speed are the significant parameters and along Z-direction beam speed, hatch spacing and part bed temperature are found to be most significant factors influencing shrinkage. Empirical models for predicting shrinkage along X, Y and Z directions are derived using regression. Obtained results are validated and they are found in good agreement with experiments. One case study of bench marking part is also presented to show that shrinkage model developed in the present work confine more accurate parts.

Keywords: Selective laser sintering; Shrinkage; Taguchi method; S/N ratio; ANOVA

1. Introduction

Rapid prototyping (RP) or layered manufacturing (LM) is the third phase in the evolution of prototyping after manual and virtual prototyping. RP is used to fabricate a physical (three-dimensional) object of any shape directly (usually a CAD model) from numerical data by a quick, highly automated and totally flexible process. It is an important technology as it has potential to reduce the manufacturing lead time of the product up to 50%, even the relative part complexity is very high [1,2]. The commercial RP systems available today are Stereolithography (SL), selective laser sintering (SLS), fused deposition modelling (FDM), laminated object manufacturing (LOM) and three-dimensional printing (3DP), etc.

SLS is a RP technology that allows generating complex 3D parts layer by layer [3]. A CAD model is first tessellated and sliced into layers of 0.05–0.3 mm thickness. SLS uses fine powder which is spread by a re-coater on the machine bed and scanned selectively by a CO_2 laser of power 25–50 W such that the surface tension of the grains is overcome and they are sintered together. Before the laser is scanned, entire machine bed is heated to just below the melting point of the material by infra red heaters to minimize thermal distortion and to facilitate fusion to the previous layer. Laser power is adjusted to bring the selected powder areas to a temperature just sufficient for the

*Corresponding author. Tel.: +91 1126596083; fax: +91 1126582053.
E-mail address: pmpandey@mech.iitd.ac.in (P.M. Pandey).

0890-6955/$ - see front matter © 2006 Elsevier Ltd. All rights reserved.
doi:10.1016/j.ijmachtools.2006.07.001

Nomenclature

B_S	Beam speed (mm/s)
C.I.	Confidence interval
D_{CAD}	Desired dimension of CAD model
D_{DSM}	Dimension obtained by using of developed shrinkage models
D_{SMM}	Dimension obtained when shrinkage factors suggested by machine manufacturer are used
DOF_e	Degrees of freedom of error term
DOF_m	Degrees of freedom of mean (always 1)
F	Fisher value
η	Signal-to-Noise (S/N) ratio
H_s	Hatch spacing (mm)
I_a	Index for improvement in accuracy of a dimension
l	Number of parameter levels
L_c	Original CAD model dimension (mm)
L_m	Measured dimension on the specimen (mm)
L_P	Laser power (watt)
L_S	Scan length (mm)
m	Overall mean S/N ratio
M.S.D.	Mean square deviation
MS_e	Mean square of error term
MS_j	Mean square of factor
n	Total number of experiments
N_e	Effective number of replications
n_p	Number of significant parameters
ρ	Percentage contribution
S_i^*	Mean shrinkage (%) of ith parameter at optimal level
S_m	Overall mean shrinkage (%)
S_{opt}	Shrinkage (%) at optimal level of parameters
SS_e	Sum of squared error
SS_j	Sum of squared deviations for each design parameter
SS_T	Total sum of squares
S_X	Shrinkage (%) in X-direction
S_Y	Shrinkage (%) in Y-direction
S_Z	Shrinkage (%) in Z-direction
T_B	Part bed temperature (°C)
V_e	Variance of error term
Y	Mean shrinkage (%)

powder particles to get sintered. After allowing sufficient time for the sintered layer to cool down without causing significant internal stresses, the part bed moves down by one layer thickness to facilitate new powder layer, spread by a re-coater. The sintered material forms the part while the un-sintered powder remains in its place to support the structure and may be cleaned away and recycled once the build is complete. SLS can be used to process any material, provided it is available in the form of powder and that the powder particles tend to fuse or sinter when heat is applied [4]. The powder materials that can be sintered are polymers, reinforced and filled polymers, metals and ceramics.

Nowadays, RP is emerging as a rapid manufacturing technique, which produces the functional parts in small batches, particularly in aerospace application and rapid tooling. Therefore, there is a need that RP prototypes should have high accuracy in order to ensure proper functional requirements. However, the accuracy of an RP process is difficult to predict as it is a function of many different factors, some of which are interdependent also. The factors that influence accuracy of RP prototypes are accuracy of tessellation from the CAD model, slicing algorithm, data transfer, device motion resolution, powder granulometry, beam offset and the shrinkage [5,6]. One of the major causes of part inaccuracy in SLS is shrinkage during sintering [5,7] which does not occur in a uniform manner. The shrinkage of a new layer can be constrained by the existing part substrate. In addition, areas at high temperatures tend to shrink more than those at lower temperatures and part geometries such as thick walls or sections can increase the shrinkage. To compensate for shrinkage, a material shrinkage coefficient is calculated and a scaling factor is applied in each direction to the STL file [7]. The resulting geometry can be slightly oversized compared with the nominal geometry, depending on the scaling factor used.

Several attempts have been made to improve the accuracy of the RP parts by controlling the effect of shrinkage. Wang [5] discussed the two most important parameters namely shrinkage and beam offset for the SLS process. Formula for shrinkage and beam offset has been derived in his work which can be used for scaling up the CAD models.

Nelson et al. [8] developed a one-dimensional heat transfer model of SLS process for predicting sintering depths in polycarbonate powders. They also conducted experimental studies to validate their simulation findings.

Williams and Deckard [9] used analytical and experimental methods to study the effect of energy density, spot diameter and delay on average density and strength of SLS parts. Their findings show that with the increase in energy density and spot diameter there is increase in density and strength of SLS prototypes. However there exists a range of delay time which gives maximum density and strength. This paper does not deal directly with the shrinkage or defects of SLS prototypes.

Wang et al. [10] investigated the relationship between post-cure shrinkage and the various process parameters for Stereolithography by using least-square method. They concluded that, as the curing degree of the green-state prototype increases, the shrinkage encountered reduces. They also found that curing degree is a function of laser power, layer pitch, scan pitch and scanning speed.

Childs et al. [11] analyzed the thermal and powder densification of SLS process for amorphous polycarbonate. Their analysis showed that the densification and linear accuracy due to sintering were mostly sensitive to changes in the activation energy and heat capacity of the polymer. Powder bed density and the powder layer thickness were included as secondary factors for the linear accuracy.

Yang et al. [12] proposed compensation test pieces for the X, Y, and Z-axes to compensate for the shape distortions caused by phase changes during the sintering process and the shrinkage rates have been measured experimentally. With those shrinkage rates, a set of equations is proposed that give the scale factors of the X, Y, and Z-axes. The scale factors obtained from the proposed building compensation test pieces of X, Y, and Z-axes satisfy the required dimensional accuracy even if there are changes in the build positions and in the size of the SLS parts. Their work is mainly focused on study of location of part on part bed and does not aim at shrinkage variation with process parameters.

Dai and Shaw [13] proposed a finite element analysis to investigate the effect of laser scanning patterns on residual thermal stresses and distortion. They concluded that the out-of-plane distortion of a layer, processed by a moving laser beam can be minimized with a proper selection of the laser scanning pattern. They also reported that the scanning pattern which has its long scanning direction parallel to one axis, leads to a saddle-shaped distortion. Along the long scanning direction, distortion is concave downward, whereas concave upward in the perpendicular direction.

Ning et al. [14] proposed an intelligent parameter selection system for direct metal laser sintering (DMLS) process. Their system assists users to choose the optimum parameter values for processing time, mechanical properties, geometric accuracy and surface roughness. They developed a model based on the feed forward neural network with back propagation learning algorithm to achieve better mapping between process parameters and part properties. The system developed can determine the most suitable parameter settings containing the process parameters and predict resulting properties from the database built based on different process requirements automatically.

Wenbin et al. [15] presented finite element simulation for stair stepping effect caused by material shrinkage through layer-by-layer manner in RP processes. They reported that the layers had a small initial expansion before a large shrinkage. They concluded that the light intensity does not have significant effect on staircase control. The decrease in layer thickness affects the stair stepping significantly.

Ning et al. [16] conducted series of experiments for DMLS process to find the effect of hatch length on the material anisotropy, heterogeneity and part strength. They concluded that short hatch lines result serious shrinkage and become less homogeneous.

It is evident from the literature review presented above that part accuracy is affected highly by shrinkage. Laser power, beam speed and layer thickness have significant effect on the shrinkage in Stereolithography [10]. Ning et al. [16] proposed an algorithm to find out optimal hatch direction for a typical layer by considering the shrinkage as a function of hatch length. Many researchers [5,12,13,15,16] concentrated on studying the accuracy and distortion in SLS process either by using finite element analysis or by suggesting a factor in X, Y and Z directions for scaling up the STL file. No attempt appears to be made in author's knowledge for studying effect of process parameters on shrinkage for SLS process which is a major cause of inaccuracy. Therefore, the present work aims on finding out the effect of parameters namely laser power, beam speed, hatch spacing, part bed temperature and scan length on shrinkage for better accuracy. Experiments are planned by using Taguchi's L_{16b} orthogonal array. Percentage difference in the dimensions of CAD model and fabricated prototype along X, Y and Z-axes are considered as responses. S/N ratio and ANOVA is used to analyze the main effects and to obtain the optimum parameter for maximum accuracy. Regressions models of percentage shrinkage along X, Y and Z-axes are developed to scale up the STL file for better accuracy. A confirmation experiment is conducted to validate the developed models at optimum level of parameters. Case study of a benchmarking component is also presented to gain confidence.

2. Planning of experiments

Experiments are planned by using Taguchi method as it is considered to be a powerful tool when a process is affected by number of parameters. In classical methods of experimental planning (factorial designs, fraction factorial designs, etc.) a large number of experiments have to be carried out as the number of the process parameters increases, which is difficult and time consuming and also results in higher cost as it is the case with RP. To solve this problem, Taguchi proposed an experimental plan in terms of orthogonal array that gives different combinations of parameters and their levels for each experiment [17,18]. According to this technique, entire parameter space is studied with minimum number of experiments. A brief description of Taguchi method is presented below.

2.1. Taguchi method

Taguchi approach uses three major steps namely system design, parameter design and tolerance design for optimizing a process or product. In system design, scientific and engineering knowledge is applied to produce a basic functional prototype design. It contains selection of materials, components, production equipment, process parameter values, etc. Next to the system design is the parameter design, which is used to optimize the settings of process parameter values for improving quality characteristics. Final step of the optimization is tolerance design, used to determine and analyze tolerances around the optimal settings recommend by the parameter design

[17,18]. To improve the accuracy in SLS process, parameter design proposed by Taguchi is adopted in present work for modeling of shrinkage.

2.2. Details of experiments

Cuboids having 30×30 mm cross section with different lengths (which is same as scan length) are selected as the specimens. The material used in the present work is polyamide powder with refresh rate of 30:70 fresh and used powders. Ranges of laser power, beam speed and hatch spacing are chosen based on the maximum energy density (given below) because higher energy density causes degradation of the material.

$$E = \frac{P}{V \times H_s}, \tag{1}$$

where E is Energy density J/mm^2, P is Laser power in W, V is beam speed in mm/s and H_s is Hatch spacing in mm. From our experience the sintering does not occur if value of E is below 1 J/cm^2 and polymer degradation starts above 4.8 J/cm^2. Therefore range of the laser power, beam speed and hatch spacing are selected as 24–36 W, 3000–4500 mm/s and 0.22–0.28 mm, respectively. Phenomenon of curling is observed when the part bed temperature is less than 175 °C and if it is beyond 178 °C, caking occurs. Caking is a phenomenon in which the powder particles stick together and large amount of the powder forms as lump and it moves with recoater. Range of scan length is suitably selected and is same as length of the part along X-direction. The laser spot size has been kept fixed and is same as 0.6 mm. various levels of different parameters used in the present work are given in Table 1.

In present study, L_{16B} orthogonal array [18] with five columns and sixteen rows is used and is given in Table 2. To select an appropriate orthogonal array, total degrees of freedom need to be computed. The degrees of freedom are the number of comparisons to be made between design parameters. For example, a four-level design parameter counts for three degrees of freedom. Therefore, in the present work, total degrees of freedom are 16, 15 owing to 5 parameters with four levels and one for overall mean [18]. Basically, degrees of freedom for an orthogonal array should be greater than or at least equal to number of design parameters. Each parameter is assigned to each column of the orthogonal array, so 16-parameter combinations are available. Therefore, only 16 experiments are required to study the entire parameter space using L_{16B} orthogonal array.

Specimens are modeled in Pro/Engineer® and exported as STL files. These STL files are imported to Magics software without scaling for shrinkage, and the positions, building orientation of specimens are fixed. Then the STL files are checked for errors and repaired. Once the orientation and position are fixed, the specimens are imported to the RP tools software and sliced into layers of 0.15 mm thickness. Sliced file is then corrected (repairing the errors) and transferred to the machine. Specimens are produced in four sets, with different part bed temperature in every set. Specimens are placed near the center of part bed (as shown in Fig. 1) and scanned along X-direction. The produced specimens are shown in Fig. 2. Dimensions of fabricated specimens are measured by using screw gauge (least count 0.01 mm) along X, Y and Z directions. Each dimension is measured three times and the average is considered. Shrinkage (%) for each of the specimen in a direction is calculated by using the following Equation [16]:

$$\text{Percentage shrinkage} = \frac{L_c - L_m}{L_c} \times 100, \tag{2}$$

Table 2
Taguchi L_{16B} orthogonal array

Experiment No.	Columns				
	Factor 1	Factor 2	Factor 3	Factor 4	Factor 5
1	1	1	1	1	1
2	1	2	2	2	2
3	1	3	3	3	3
4	1	4	4	4	4
5	2	1	2	3	4
6	2	2	1	4	3
7	2	3	4	1	2
8	2	4	3	2	1
9	3	1	3	4	2
10	3	2	4	3	1
11	3	3	1	2	4
12	3	4	2	1	3
13	4	1	4	2	3
14	4	2	3	1	4
15	4	3	2	4	1
16	4	4	1	3	2

Table 1
Levels of each of the parameters

S. No.	Parameter	Levels of each parameter			
		Level 1	Level 2	Level 3	Level 4
1	Laser power (W)	24	28	32	36
2	Scan speed (mm/s)	3000	3500	4000	4500
3	Hatch spacing (mm)	0.22	0.24	0.26	0.28
4	Part bed temperature (°C)	175	176	177	178
5	Scan length (mm)	30	45	60	75

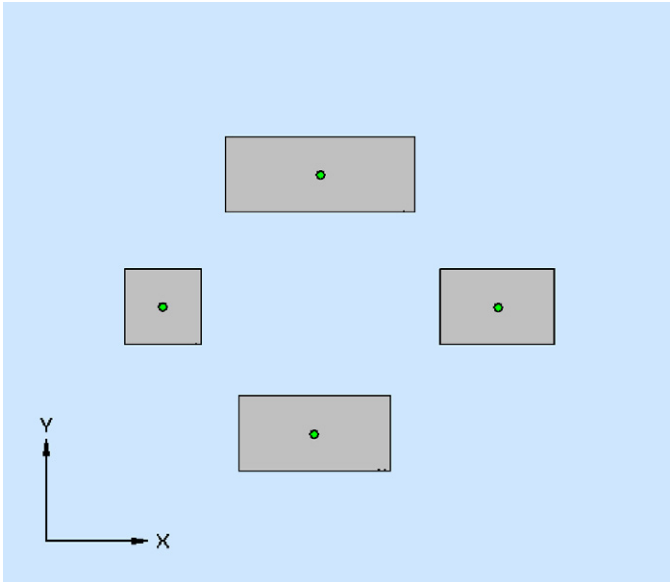

Fig. 1. Arrangement of the specimens in Magics software.

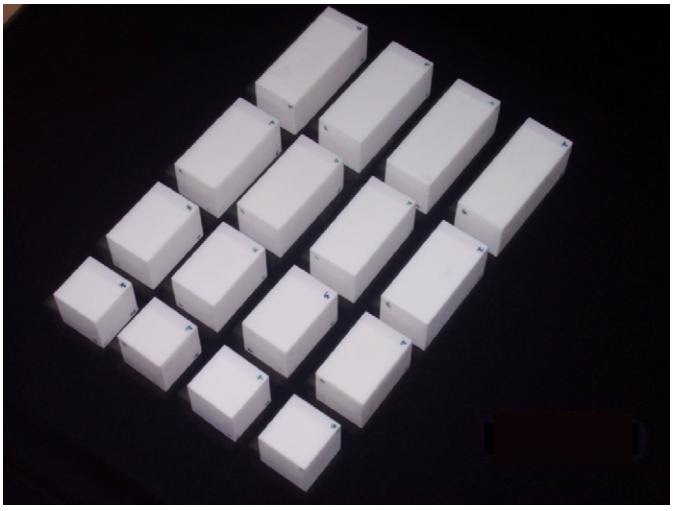

Fig. 2. Specimens produced on EOSINT P 380 SLS work station, Indian Institute of Technology Delhi.

where L_c is the original dimension of CAD model and L_m is the measured dimension.

2.3. Analysis of experimental data

Experiments data is analyzed by using S/N ratio and ANOVA. Based on the results of the S/N ratio and ANOVA, optimal parameter settings for better accuracy are obtained and verified experimentally. Regression models are developed to get the compensation factor for any set of process parameters.

2.3.1. Analysis using S/N ratio

In Taguchi method, S/N ratio is measure of quality characteristics and deviation from the desired value. The term signal represents the desirable value (mean) and the noise represents the undesirable value (Standard Deviation from Mean) for the output characteristic [17]. The S/N ratio (η) is defined as

$$\eta = -10 \log(\text{M.S.D.}), \tag{3}$$

where M.S.D. is the mean-square deviation for the output characteristic. Shrinkage is the dominant phenomenon in SLS which causes deviation of dimensions from desired dimension (CAD model). Parts can be built with better accuracy if the shrinkage effect is reduced. So, smaller the better type of S/N ratio is used in analysis for better accuracy. For smaller the better case, the S/N ratio is obtained by [17]

$$\text{M.S.D.} = \frac{1}{n}\sum_{i=1}^{n} Y_i^2, \tag{4}$$

where n is the total number of the experiments in the orthogonal array and Y_i is the mean percentage shrinkage for the ith experiment.

S/N ratio for each of the experiment is calculated and is presented in Table 3. The effect of a factor level is defined as the deviation it causes from the overall mean. The overall mean S/N ratio (m) of the experiments is calculated by [17]

$$m = \frac{1}{n}\sum_{i=1}^{n} \eta_i, \tag{5}$$

where η_i is the mean S/N ratio of the ith experiment.

All four levels of every factor are equally represented in 16 experiments. Thus m is a balanced overall mean for the entire experiment. Since the experimental design is orthogonal, it is possible to separate out the effect of each factor at each level [18]. Mean response is the average of quality characteristic for each parameter at different level. S/N ratio and shrinkage (%) for each parameter at each level can be calculated from mean S/N ratio and shrinkage (%) value of each of the experiment. For example, the mean percentage shrinkage for beam speed at level 1 can be calculated by averaging shrinkage (%) from the experiments 1, 5, 9 and 13. Shrinkage (%) for each of the parameter at each level is calculated. These are also called as main effects. Figs. 3–5 show the shrinkage (%) response (main effects) along X, Y and Z directions, respectively. The ideal product or process will only respond to the operator's signals and will be unaffected by random noise factors. Therefore, S/N ratio is to be maximized. Based on the S/N analysis, the optimal parameters for minimum shrinkage are given in Table 4.

From main effect plots (Figs. 3–5) it is observed that there is reduction in shrinkage as the energy density is increased. Increase in energy density causes increase in depth and width of the laser scan line [10]. Therefore, the dimensions of the sintered part are slightly oversize and come closer to the desired dimensions after cooling. Increase in energy density also causes increase in temperature at curing area, which

Table 3
S/N ratio and shrinkage (%) for each of the experiments in *X*, *Y* and *Z* directions

Experiment no.	*X*-direction		*Y*-direction		*Z*-direction	
	S/N ratio	Average shrinkage (%)	S/N ratio	Average shrinkage (%)	S/N ratio	Average shrinkage (%)
1	1.9856	0.79167	3.6123	0.65833	−8.4658	2.65
2	2.7250	0.72778	0.3595	0.95	−9.3486	2.93333
3	2.1814	0.775	−2.4069	1.31667	−11.2063	3.63333
4	3.5019	0.66667	−3.5486	1.5	−12.0804	4.01667
5	8.5817	0.37	4.1927	0.60833	−10.2560	3.25
6	6.1966	0.47917	1.3767	0.85	−10.0582	3.18333
7	6.8060	0.45556	5.2489	0.54167	−9.3982	2.95
8	−1.0965	1.13333	−1.2809	1.15833	−10.8053	3.46667
9	4.8655	0.56667	2.3471	0.75833	−10.3493	3.29167
10	0.8252	0.90833	−1.5288	1.19167	−9.8275	3.1
11	8.0208	0.39667	3.8166	0.64167	−9.5467	3.0
12	5.0515	0.55833	−0.7828	1.09167	−9.8779	3.11667
13	7.9948	0.39583	8.3039	0.38333	−9.0737	2.84167
14	10.2626	0.30667	3.8195	0.63333	−9.4947	2.98333
15	2.0528	0.78333	1.1429	0.875	−9.8045	3.09167
16	4.1754	0.61667	4.1329	0.61667	−10.4374	3.325

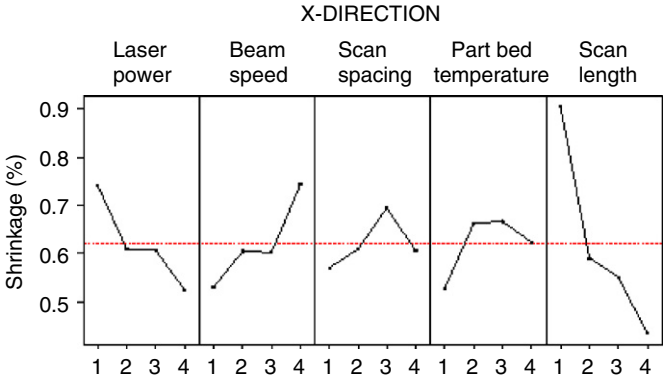

Fig. 3. Effect of process parameters on shrinkage in *X*-direction.

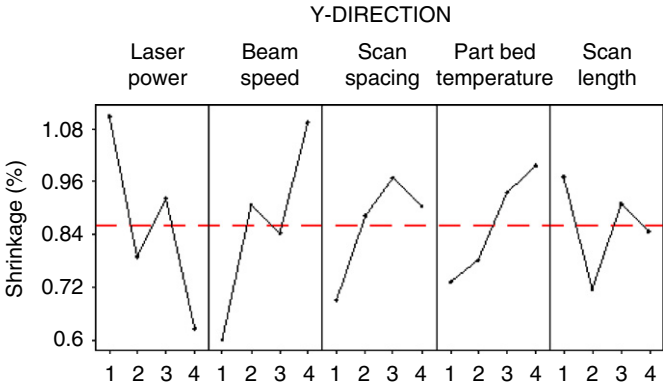

Fig. 4. Effect of process parameters on shrinkage in *Y*-direction.

leads to the reduction in amount of crystallinity [19,20]. Reduction of crystallinity causes decrease in shrinkage. The same trend has been reported by Wang et al. [10] for Stereolithography process when photopolymer is used.

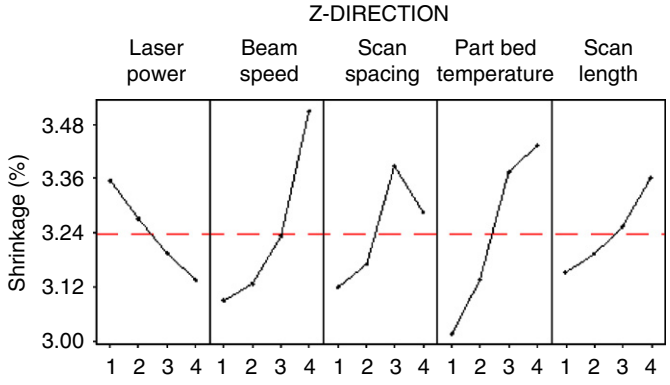

Fig. 5. Effect of process parameters on shrinkage in *Z*-direction.

Table 4
Optimum process parameter values for minimum shrinkage obtained from S/N ratio

S. no.	Parameter	Unit	Value
1	Laser power	W	36
2	Beam speed	mm/s	3000
3	Hatch spacing	mm	0.22
4	Part bed temperature	°C	175

William and Deckard [9] reported that there is increase in prototype density with increase in energy density but they have not reported anything about shrinkage explicitly. William and Deckard [9] have also not used variations in crystallinity in their computational/mathematical model due to change in temperatures which may be a major cause of reduction in shrinkage. The reasons for increase in density in experimental work as reported by William and Deckard [9] with Andrew number may be due to the reason that effect of fusion of polycarbonate particles while sintering is more

effective at higher temperature ranges as compared to reduction of crystallinity while cooling which causes reduction in shrinkage [19] as the energy density used in their work (40–180 kJ/m^2) which is approximately 4–5 times as compared to energy density (10–48 kJ/m^2) used in the present work. The two polymers, i.e., polycarbonate and polyamides also posses different properties at different temperature ranges. Increase in part bed temperature reduces the cooling rate which allows time for the molecules to arrange in an order, which results increase in crystallinity. Increase in crystallinity causes increase in shrinkage. Shorter hatch lines results in more serious shrinkage along hatching (X) direction. When the scan length is small, the sintered powder does not have sufficient time to cool as it absorbs energy transferred from the neighboring scan lines [16]. Therefore, low cooling rate causes the increase in shrinkage. It is observed that shrinkage (%) is more in Z direction than X and Y directions and is probably due to the weight of the successive layers. Shrinkage is not identical along X, Y and Z axes because laser scanning is done along X direction and the part is built along Z direction.

2.3.2. Analysis of variance

ANOVA is a standard statistical technique to interpret the experimental results. It is extensively used to identify the performance of group of parameters under investigation. Purpose of ANOVA is to investigate the parameters, whose combination to total variation is significant. In ANOVA, total sum of squares (SS_T) is calculated by [17]

$$SS_T = \sum_{i=1}^{n} (\eta_i - m)^2, \tag{6}$$

where m is the overall mean S/N ratio.

Total sum of squared deviations SS_T is divided into two sources [17]

$$SS_T = \sum_{j=1}^{n_p} SS_j + SS_e, \tag{7}$$

where SS_j is the sum of squared deviations for each design parameter and is given by

$$SS_j = \sum_{i=1}^{l} (\eta_{ji} - m)^2, \tag{8}$$

here n_p is the number of significant parameters and l is the number of levels of each parameter. SS_e is the sum of squared error without or with pooled factor, which is sum of squares corresponding to the insignificant factors. Mean square of a factor (MS_j) or error (MS_e) is found by dividing its sum of squares with its degrees of freedom. Percentage contribution (ρ) and F-value of each of the design parameters is given by [17]

$$\rho_j = \frac{SS_j}{SS_T}, \tag{9}$$

$$F_j = \frac{MS_j}{MS_e}. \tag{10}$$

If the factor is highly influencing the process response, then the F-value is large and is used to rank the factors [17]. The obtained F-values for shrinkage in X, Y and Z directions in the present work are given in Tables 5–7. It can be seen form Table 5 that scan length and laser power are the most significant parameters for shrinkage in X direction. Laser power and beam speed are the most significant parameters affecting the shrinkage in Y direction as given in Table 6. Part bed temperature, beam speed and hatch spacing are the significant parameters for shrinkage in Z direction (Table 7).

2.4. Empirical model derivation

For each combination of parameter settings in L_{16B} matrix, percentage shrinkage values in X, Y and Z directions are already tabulated (Table 3). Empirical models are derived by linear regression using standard statistical software. Insignificant (pooled) parameters are neglected while deriving these models. The developed models predict the shrinkage (%) for any set of parameters to scale up the STL file for better accuracy. These scaling factors (S_X, S_Y and S_Z in %) to compensate shrinkage along X, Y and Z directions are as given below.

$$S_X = 1.611691 - 0.01615\,L_P - 0.009647\,L_S, \tag{11}$$

$$S_Y = 0.785926 - 0.032656\,L_P + 0.000281\,B_S, \tag{12}$$

$$S_Z = -28.6238 + 0.000308\,B_S + 4.0417\,H_S + 0.16792\,T_B, \tag{13}$$

Table 5
ANOVA table for shrinkage in X-direction

S. no.	Factor	DOF	Sum of square	Mean square	F	Contribution (%)
1	Laser power	3	26.3879	8.796	2.51	0.176
2	Beam speed	3	18.5087[a]	6.1696		
3	Hatch spacing	3	2.2892[a]	0.7631		
4	Part bed temperature	3	10.7962[a]	3.5987		
5	Scan length	3	91.6087	30.5362	8.7	0.612
6	Total	15	149.5907			
7	Error	6	31.595	3.551		

[a]Indicates the minimum mean square values of pooled parameters as their % contribution is low.

Table 6
ANOVA table for shrinkage in *Y*-direction

S. no.	Factor	DOF	Sum of square	Mean square	*F*	Contribution (%)
1	Laser power	3	51.2587	17.0862	3.141	0.334
2	Beam speed	3	53.1145	17.7048	3.255	0.346
3	Hatch spacing	3	15.5203[a]	5.1734		
4	Part bed temperature	3	20.1395[a]	6.7131		
5	Scan length	3	13.2939[a]	4.4313		
6	Total	15	153.3269			
7	Error	3	48.9537	5.4393		

[a]Indicates the minimum mean square values of pooled parameters as their % contribution is low.

Table 7
ANOVA table for shrinkage in *Z*-direction

S. no.	Factor	DOF	Sum of square	Mean square	*F*	Contribution (%)
1	Laser power	3	0.7636[a]	0.2545		
2	Beam speed	3	3.8263	1.2754	4.77	0.337
3	Hatch spacing	3	1.5803	0.5268	1.97	0.139
4	Part bed temperature	3	4.3442	1.4481	5.41	0.383
5	Scan length	3	0.8415[a]	0.2805		
6	Total	15	11.3559			
7	Error	6	1.6051	0.2675		

[a]Indicates the minimum mean square values of pooled parameters as their % contribution is low.

where L_P is the laser power in W, B_S is the beam speed in mm/s, H_S is the hatch spacing in mm, T_B is the part bed temperature in °C and L_S is the scan length in mm.

2.5. Confirmation test

Confirmation experiment is carried out to validate the developed empirical models. Levels of process parameters selected for the confirmation test are optimum parameters as given in Table 4. The estimated shrinkage (%) using the optimal level of the design parameters is expected to fall in the range given below [21].

$$\text{Expected shrinkage} = S_{\text{opt}} \pm \text{C.I.}, \tag{14}$$

where

$$S_{\text{opt}} = S_{\text{m}} + \sum_{i=1}^{n_{\text{p}}} \left(S_i^* - S_{\text{m}}\right) \tag{15}$$

and confidence interval

$$\text{C.I.} = \left[\frac{F_{(1,\text{DOF}_{\text{e}})} \times V_{\text{e}}}{N_{\text{e}}}\right]^{0.5}. \tag{16}$$

In the above three Eqs. (14)–(16), S_{m} is the overall mean shrinkage, S_i^* is the mean shrinkage (%) at the optimal level, n_{p} is the number of main design parameters that affect the quality characteristic, $F_{(1,\text{DOE}_{\text{e}})}$ is Fisher value at DOF_{e} which is degrees of freedom of error term and V_{e} is the variance of the error term. Effective number of replications (N_{e}) is given by [21]

$$N_{\text{e}} = \frac{n}{\text{DOF}_{\text{m}} + \sum_{\text{i}=1}^{n_{\text{p}}} \text{DOF}_i}, \tag{17}$$

where DOF_{m} is the degrees of freedom of mean which is always 1 and DOF_i is the degrees of freedom of the significant parameters.

The expected shrinkage (%) at optimal set of parameters is calculated from Eqs. (14)–(17). Table 8 and Fig. 6 shows the comparison of the expected shrinkage predicted from Eqs. (14)–(17) at 90% confidence level with the measured shrinkage value of confirmation experiment. Good agreement between the expected and actual shrinkage is observed. However, the range of the expected shrinkage in *Y*-direction is more. This is probably due to some other factor or interaction, which is not considered in present study is also influencing shrinkage in *Y*-direction. Experimental results confirm the effectiveness of the prior design and analysis for relating the process parameters with shrinkage (%) in SLS.

3. Case study

One benchmarking part is fabricated and measured for accuracy to gain confidence. The bench marking part shown in Fig. 7 has been suggested in literature [22] for SLS. This part is fabricated in two sets. In first set, the part is fabricated at the parameters and scaling factors suggested by machine manufacturer for better accuracy.

Table 8
Comparison of shrinkage (%) predicted by ANOVA and confirmation experiment

S. no.	Direction	Shrinkage (%)		
		From Eqs. ((11)–(13))	Expected range of values from ANOVA at confidence level of 90%	Measured value from confirmation experiment
1	*X*	0.4843	0.1684–0.5115	0.4667
2	*Y*	0.2113	0.0837–0.6529	0.2667
3	*Z*	2.575	2.2967–2.9407	2.25

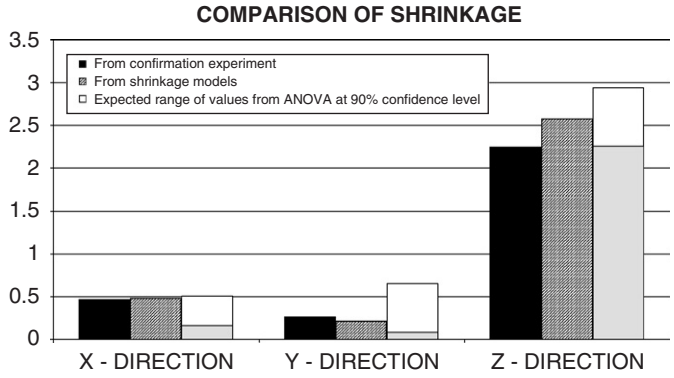

Fig. 6. Comparison of shrinkage (%) obtained experimentally and predicted by ANOVA.

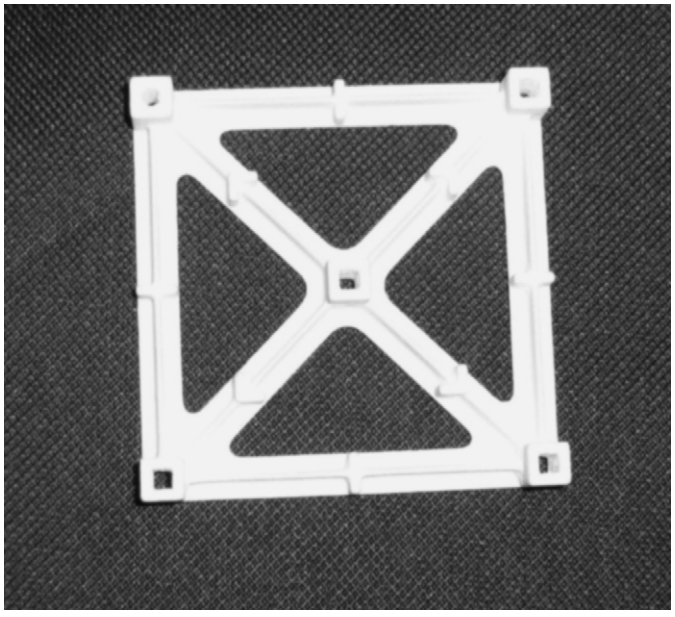

Fig. 7. Bench marking part (considered in literature [22]) fabricated to compare the shrinkage between standard method and developed models.

In second set part is fabricated with parameters suggested by machine manufacturer (given in Table 9) for better accuracy and corresponding scaling factors are calculated using developed models (Eqs. (11)–(13)). These scaling factors are applied to STL file of part to be manufactured by using standard scaling transformation. Bench marking part is also fabricated at optimum set of parameters

Table 9
Process parameters suggested by machine supplier for better accuracy

S. no.	Parameter	Unit	Value
1	Laser power	W	36
2	Beam speed	mm/s	4500
3	Hatch spacing	mm	0.30
4	Part bed temperature	°C	175

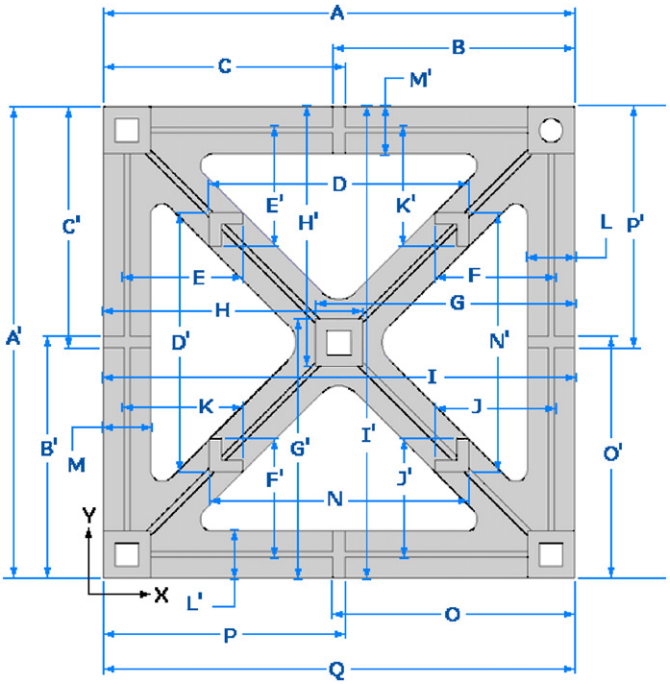

Fig. 8. Dimensions selected for comparison.

predicted by ANOVA (Table 4) and corresponding scaling factors from the developed models. Typical dimensions of the part (shown in Fig. 8) are measured and compared with the desired (CAD model) dimensions. The comparison of dimensions of the part with CAD model dimensions is given in Table 10. The index of improvement in accuracy (I_a) for a dimension of a part can be defined by

$$I_a = 1 - \frac{|D_{CAD} - D_{DSM}|}{|D_{CAD} - D_{SMM}|}, \tag{18}$$

where D_{CAD} is dimension desired by CAD model, D_{DSM} is dimension obtained by use of developed shrinkage models

Table 10
Comparison of dimensions and accuracy of bench mark part shown in Fig. 8

S. no.	Dimension	Dimension on CAD model in mm	Measured dimensions (in mm) on the parts produced by using			I_a for parameters suggested buy machine manufacturer	I_a for optimum parameters
			Parameters suggested by machine supplier for better accuracy		Optimal parameters with developed models		
			Standard method	Developed shrinkage model			
1	A	60	59.96	60.00	60.00	1.00	1.00
2	B	30.375	30.58	30.46◆	30.44	0.59	0.68
3	C	30.375	30.6	30.44	30.44	0.71	0.71
4	D	33	32.88	33.00	33.00	1.00	1.00
5	E	15.118	14.98	15.04	15.06	0.43	0.58
6	F	15.118	14.94	15.04	15.10	0.56	0.90
7	G	33	32.96	32.98	32.96	0.50	0.00
8	H	33	32.88	33.96	32.94◆	0.67	0.50
9	I	60	59.82	60.02	60.00	0.89	1.00
10	J	15.118	15	15.10	15.04◆	0.85	0.34
11	K	15.118	14.96	15.04◆	15.06	0.51	0.63
12	L	6	5.78	5.98	6.00	0.91	1.00
13	M	6	5.82	5.96	6.00	0.78	1.00
14	N	33	32.88	33.02	33.00	0.83	1.00
15	O	30.375	30.5	30.48◆	30.42	0.16	0.64
16	P	30.375	30.54	30.46◆	30.44	0.48	0.61
17	Q	60	59.86	60.06	60.04	0.57	0.71
18	A^1	60	59.92	60.08*	59.92*	0.00	0.00
19	B^1	30.375	30.54	30.40	30.40	0.85	0.85
20	C^1	30.375	30.52	30.40	30.40	0.83	0.83
21	D^1	33	32.96	33.04	32.96	0.00	0.00
22	E^1	15.118	15.02	15.02*	15.04*	0.00	0.20
23	F^1	15.118	15.02	15.06	15.08	0.41	0.61
24	G^1	33	32.9	33.04	32.94	0.60	0.40
25	H^1	33	32.88	33.00	32.92	1.00	0.33
26	I^1	60	59.62	60.10*	59.88*	0.74	0.68
27	J^1	15.118	15.04	15.04	15.10	0.00	0.77
28	K^1	15.118	15.02	15.06	15.06	0.41	0.41
29	L^1	6	5.86	6.00	5.94	1.00	0.57
30	M^1	6	5.84	6.00	5.96	1.00	0.75
31	N^1	33	32.86	33.04	32.92*	0.71	0.43
32	O^1	30.375	30.58	30.48*	30.46	0.49	0.59
33	P^1	30.375	30.58	30.48*	30.50*	0.49	0.39

and D_{SMM} is dimension obtained when shrinkage factors suggested by machine manufacturer are used. From Table 10 it can be observed that the part produced using developed models are more accurate than the part fabricated using scaling factor suggested by machine manufacturer.

It can be seen from Table 10 that the difference between CAD model dimensions and the dimensions of the fabricated parts is slightly higher at some places (indicated with ◆, along *X*-direction at B, H, J, K, O and P in Table 10). This is probably due to the reason that scan length is variable but while predicting the values of shrinkage an average scan length is considered. It can be observed from Table 10 (at A^1, E^1, I^1, N^1, O^1 and P^1) that the difference between CAD model dimensions and the dimensions of the fabricated parts is also slightly higher (indicated with * along *Y*-direction.). This is probably due to non-consideration of an interaction term or some other variable which may be influencing shrinkage in this direction. Further it is also observed that certain parts fabricated with optimum parameters are more accurate in *X* and *Y* directions, however slight discrepancy is observed in dimensions along *Z* direction. This is due to distortion resulting from high-energy density. It is also observed that some unsintered powder gets stick to the prototype fabricated at optimal set of parameters and is due to over sintering. Overall, the parts fabricated by using scaling factors calculated from the developed shrinkage models are found to be more accurate.

4. Conclusions

In present work, the relationship between the shrinkage and various process parameters namely laser power, beam speed, hatch spacing, part bed temperature and scan length is developed. Cuboids are selected as specimens rather than

long strips along X, Y and Z directions as it is expected that the shrinkage along X, Y and Z direction is not independent. Taguchi method is adopted for the design of experiments and analysis of experimental data is done successfully by maximizing S/N ratio and ANOVA. Prediction of developed models is in good agreement with experimental findings. One case study is successfully presented to show the effectiveness of developed models for improving the accuracy of SLS prototypes. The use of findings of Yang et al. [12] along with this work increases the usefulness of the two attempts.

References

[1] D.T. Pham, S.S. Demov, Rapid Manufacturing: The technologies and applications of Rapid Prototyping and Rapid Tooling, Springer, London Limited, 2001.

[2] C.K. Chua, K.F. Leong, Rapid Prototyping: Principles and Applications in Manufacturing, Wiley, 1997.

[3] P.K. Venuvinod, W. Ma, Rapid Prototyping: Laser Based and other Technologies, Kluwer Academic Publishers, 2004.

[4] J.P. Kruth, X. Wang, T. Laoui, L. Froyen, Lasers and materials in selective laser sintering, Assembly Automation 23 (4) (2003) 357–371.

[5] X. Wang, Calibration of shrinkage and beam offset in SLS, Rapid Prototyping Journal 5 (3) (1999) 129–133.

[6] N.P. Karapatis, J.P.S. Van Griethuysen, R. Glardon, Direct rapid tooling: a review of current research, Rapid Prototyping Journal 4 (2) (1998) 77–89.

[7] D.T. Pham, S.S. Dimov, F. Lacan, Selective laser sintering: applications and technological capabilities, Journal of Engineering Manufacture 213 (1999) 435–449.

[8] J.C. Nelson, S. Xue, J.W. Barlow, J.J. Beaman, H.L. Marcus, D.L. Bourell, Model of selective laser sintering of bisphenol—a polycarbonate, Industrial Engineering and Chemical Research 32 (1993) 2305–2317.

[9] J.D. Williams, C.R. Deckard, Advances in modeling the effects of selected parameters on the SLS process, Rapid Prototyping Journal 4 (2) (1998) 90–100.

[10] W.L. Wang, C.M. Cheah, J.Y.H. Fuh, L. Lu, Influence of process parameters on Stereolithography part shrinkage, Materials & Design 17 (4) (1996) 205–213.

[11] T.H.C. Childs, M. Berzins, G.R. Ryder, A. Tontowi, Selective laser sintering of an amorphous polymer—simulations and experiments, Journal of Engineering manufacture 213 (1999) 333–349.

[12] H.J. Yang, P.J. Hwang, S.H. Lee, A study on shrinkage compensation of the SLS process by using the Taguchi method, International Journal of Machine Tools & Manufacture 42 (2002) 1203–1212.

[13] K. Dai, L. Shaw, Distortion minimization of laser processed components through control of laser scanning patterns, Rapid Prototyping Journal 8 (5) (2002) 270–276.

[14] Y. Ning, J.Y.H. Fuh, Y.S. Wong, H.T. Loh, An intelligent parameter selection system for the direct metal laser sintering process, International Journal of Production Research 42 (1) (2004) 183–199.

[15] H. Wenbin, L.Y. Tsui, G. Haiqing, A study of the staircase effect induced by material shrinkage in rapid prototyping, Rapid Prototyping Journal 11 (2) (2005) 82–89.

[16] Y. Ning, Y.S. Wong, J.Y.H. Fuh, Effect of control of hatch length on material properties in the direct laser sintering process, Journal of Engineering Manufacture 219 (2005) 15–25.

[17] W.H. Yang, Y.S. Tarng, Design optimization of cutting parameters for turning operations based on the Taguchi method, Journal of Materials Processing Technology 84 (1998) 122–129.

[18] T.P. Bagchi, Taguchi Methods Explained, Prentice-Hall of India, 1993.

[19] R.M. Ogorkiewicz, Engineering Properties of Thermoplastics, Wiley, 1970.

[20] T.H.C. Childs, A.E. Tontowi, Selective laser sintering of a crystalline and a glass-filled crystalline polymer: experiments and simulations, Journal of Engineering Manufacture 215 (2001) 1481–1495.

[21] R.K. Roy, A Primer on the Taguchi Method, Society of Manufacturing Engineers, 1990.

[22] I. Gibson, Software Solutions for Rapid Prototyping, Professional Engineering Publishing Limited and Bury St. Edmunds, UK, 2002.